AERODYNAMIC BICYCLE HELMET DESIGN USING A TRUNCATED AIRFOIL WITH TRAILING EDGE MODIFICATIONS

Bradford W Sims M.S.
University of Colorado Denver
Department of Mechanical Engineering
Denver, Colorado, United States
Phone: 530-848-1300
Email: Bradford.Sims@email.ucdenver.edu

Peter E Jenkins Ph.D., P.E.
University of Colorado Denver
Department of Mechanical Engineering
Denver, Colorado, United States
Office Phone: 303-556-2894
Email: Peter.Jenkins@ucdenver.edu

ABSTRACT

Aerodynamic drag contributes the majority of the resistance experienced by a competitive cyclist. Low aerodynamic drag is a key quality of high performance equipment and many aerodynamic helmets have been developed. These helmets are designed with a teardrop shape that attempts to maintain attached air flow. This shape provides a drag reduction when the athlete has their head up and is looking forward but has adverse effects if the athlete rotates their head down. A helmet design that helps maintain attached airflow while presenting reduced frontal area when the athlete's head is down could significantly improve performance. The aerodynamic improvements of applying a truncated airfoil shape with a trailing edge modification to a helmet design were investigated. SolidWorks Flow Simulation was used to evaluate the aerodynamic forces. A common production helmet design was progressively truncated to determine the optimal truncation length and the effects of multiple trailing edge modifications were tested. A specific truncation length with a trailing edge base cavity was found to provide similar head up performance but significantly better head down performance compared to the production design. Scale models of the final improved design and the production helmet were tested in the wind tunnel to verify the computational results.

INTRODUCTION

Aerodynamic drag contributes more than 80 percent of the resistance experienced by a cyclist traveling at 20 MPH (8.9 m/s) on flat terrain [1]. With cyclists and tri-athletes reaching speeds in excess of 30 MPH; low aerodynamic drag is a key quality of high performance equipment. Many aerodynamic helmets have been developed to reduce the aerodynamic drag experienced by cyclists. Though not optimized airfoils, current helmets are designed with a tear drop shape to try and maintain attached air flow. This shape provides a significant drag reduction when the athlete has his or her head up and is looking forward but has adverse effects if the athlete is looking down or riding in a cross-wind. A helmet design that reduces aerodynamic drag while presenting less frontal area when the athlete's head is dropped could significantly improve a cyclist's performance in real world situations.

STATEMENT OF PROBLEM

Professional tri-athletes feel current aerodynamic helmets do not meet their needs. While participating in events that have cycling sections that take 4 to 5 hours they cannot keep their head up constantly. Riding with their head down, at a negative pitch angle, negates the benefit of a traditional aerodynamic helmet by increasing frontal area and altering the drag coefficient. Figure 1 shows how the helmet frontal area increases when the pitch angle is decreased. To solve this problem we considered a movable "armadillo" style tail section of the helmet that would not stick up if the athlete dropped their head. After reviewing the federal safety standards for helmets it became evident that a moving section on the helmet would prevent it from passing the required safety tests. Subsequently alternative helmet modifications that could improve the helmet's performance for a range of head positions were investigated. Research into truncated airfoil shapes used for wind turbine blades provided inspiration for an alteration to the existing helmet design. Truncating the airfoil shape of the production helmet and adding a trailing edge modification may lead to similar aerodynamic performance at a zero pitch angle and increased performance when the athlete drops their head.

[A]

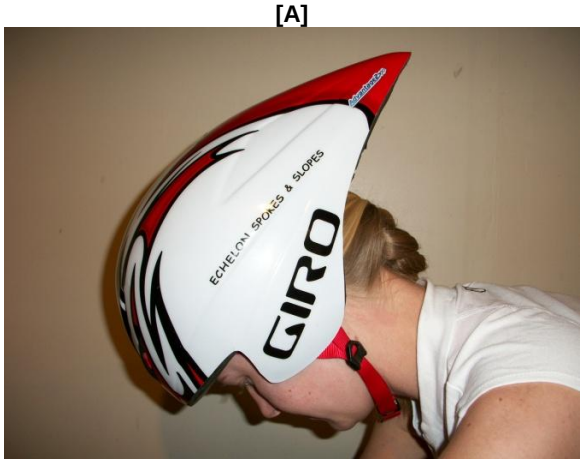

[B]

(FIGURE 1)
PRODUCTION AERODYNAMIC HELMET HEAD POSITIONS
[A] Normal head position [B] Head pitched down position

LITERATURE REVIEW

During a long bicycle time trial or during the cycling portion of a triathlon, 80 to 90 percent of the power developed by the athlete is used to overcome aerodynamic drag [1]. Many of these events are won or lost by only seconds. Small reductions in overall aerodynamic drag can easily save seconds in any of these events, giving the athlete a decisive advantage [2]. Approximately 2 to 8 percent of the athlete's total drag is a result of their helmet [1]. Helmets must provide crash protection, adequate ventilation, and reduced aerodynamic drag. In air at typical cycling speeds the Reynolds number for an aerodynamic helmet is in the range of 300,000 to 500,000. Reynolds numbers in this range show that the aerodynamic properties will be dominated by inertial effects. The aerodynamic drag resulting from surface friction is quite low compared to the resulting pressure drag. Therefore, the largest reductions in coefficient of drag can be achieved when the pressure drag is reduced by maintaining attached airflow [5].

$$R_D = 1/2 \times \rho \times A_p \times C_D \times V^2 \qquad [1]$$

The aerodynamic drag force, R_d, shown in equation [1] is dependent on ρ (air density), A_p (frontal area), C_d (coefficient of drag) and V (velocity). The drag force can be reduced by a reduction in frontal area and/or a reduction in the coefficient of drag. Production aerodynamic bicycle helmets are designed with a long tapered tail, much like an airfoil, to help maintain attached airflow. This reduces the coefficient of drag when the helmet is horizontal. As the rider tilts their head down, the helmet is pitched down, causing an increase in both the helmet's frontal area and coefficient of drag. Both these factors increase the drag force on the rider and cause a reduction in performance. During longer events it is very difficult for an athlete to keep their head up and maintain this helmet position.

Blair and Sidelko [2] performed an aerodynamic analysis of ten production aerodynamic helmets to study their performance. They also tested a standard non-aerodynamic road helmet for comparison. The tests were performed at 13.4 m/s (29.98 MPH) for three helmet pitch angles; 0, -15, and -80 degrees with respect to horizontal. At 0 and -15 degrees all ten aero helmets showed significantly lower drag than the standard helmet. At an angle of -80 degrees, nine of the aero helmets still showed a significant drag reduction compared to the standard helmet but significantly increased drag over the 0 and -15 degree positions. No individual aero-helmet showed a significantly higher reduction in drag for all angles when compared to the other helmets. Their data predicts that drag would be reduced by approximately 7.2 percent if an aerodynamic helmet, instead of a standard helmet, at a pitch angle of 0 degrees is used by a professional rider producing 450 Watts. Chabroux, Barelle, and Favier performed a similar study of six aerodynamic bicycle helmets. Their study was conducted with an air velocity of 13.9 m/s (31.1 MPH) and conducted at pitch angles of; -66.4 degrees, -36.2 degrees, and -16.8 degrees. Their results also showed that helmet inclination significantly influenced drag forces. Over all helmet angles they saw an average drag improvement of 2.4 percent over a standard non-aerodynamic helmet. They recommend reducing helmet length in order to minimize frontal area increases when the helmet is pitched down. These studies were performed in 2008 and they show that the available production helmets, of which all have similar designs, do provide a reduction in drag force but are not optimized for pitch angles lower than -20 degrees.

For athletes competing in longer cycling events, such as a 40k time trial or an Iron Man triathlon, proper head cooling is

necessary. Up to 50 percent of an athlete's heat loss comes from their head and a helmet that inhibits proper convective cooling can reduce an athlete's performance [6]. As an athlete over-heats, blood is diverted from organs and muscle to the skin in order to increase heat shedding. This is accompanied by an increase in the athlete's heart rate. Combined, these two reactions lead to a reduction in muscle performance, cardiovascular efficiency, and possible dehydration [6]. Heat loss through the head must be maximized, which makes cooling vents an essential component of an effective aerodynamic helmet. The quantity and geometry of vents can affect the aerodynamic properties of a helmet. Alam, Subic, and Akbarzadeh [1] studied the effect of vent design on standard bicycle helmet aerodynamics. Both the vent roughness (how much the vent protrudes from the helmet surface) and how vents were channeled impacted the coefficients of drag. Vent roughness showed a direct correlation with coefficient of drag. Larger, closed channel, vents were also linked to increases in drag. Chabroux, Barelle, and Favier [3] also studied the effects of vents on drag forces using three similarly shaped aerodynamic helmets. One helmet had open vents, one had small vertical slit vents, and one had no vents. Their data showed no significant difference in drag forces between the three helmets. The vents did not protrude from the helmet and they did not have complex internal channels. These two studies suggest that smaller non-protruding vents without complex channels can be used without significantly increasing drag.

Van Dam, Kahn, and Berg [4] looked at the application of truncated airfoils to the inboard region of wind turbine blades. The truncated shape provided increased lift and improved structural characteristics but also showed a significant increase in drag compared to an airfoil with a sharp trailing edge. The drag increase is a result of the low-pressure flow in the near wake of the blunt trailing edge [4]. Multiple trailing edge modifications were investigated to see how they increased base pressure and lead to reduced drag. Four main modifications were compared: a splitter plate, a trailing edge wedge, a ventilated cavity, and M shaped serrations. The slotted cavity and trailing edge wedge showed the most improvement with reductions in drag of 50 to 60 percent.

In summary, previous research has shown that helmet aerodynamics can play a significant role in performance and that production helmets do not perform well at decreased pitch angles. Current helmet design could be improved by reducing helmet length and applying a trailing edge modification.

STATEMENT OF OVERALL PURPOSE OF STUDY

The purpose of this study was to modify a production aerodynamic bicycle helmet in order to reduce the effect of head pitch angle on aerodynamic performance. A truncated airfoil shape with trailing edge modifications was applied to the helmets' design to achieve the desired results. SolidWorks solid modeling was used to design the helmet and SolidWorks Simulation was used to test the design's aerodynamic performance. The improved helmet design was compared to the production aerodynamic helmet. The method started with the 2-D analysis of the production helmet main cross-section. Truncations and trailing edge modifications were applied to the cross-section to test their effect on the drag force. The best performing combinations were then applied to the 3-D helmet design. This 3-D helmet design, on a human head model, was tested and optimized under a variety of conditions using the CFD software. To verify the 3-D CFD results a reduced scale version of the production helmet and the improved helmet were tested in the wind tunnel at the University of Colorado Denver.

EXPLANATION OF LIMITATIONS

In order to maintain a reasonable scope for the design of the helmet a few elements were not addressed. All cycling helmets are required to meet specific impact regulations. No structural analysis was made but the thickness of the helmet around the head was equal to that of the production design. No cooling vents were included in the design in order to reduce computational analysis time as well as simplify the construction of the physical models that were used in the wind tunnel. As mentioned in the literature review, small non-protruding vents with simple internal channels could be added to the design and not significantly increase the drag forces.

The helmet analysis and optimization was performed using SolidWorks Flow Simulation CFD software. Flow Simulation, like all CFD software, has distinct limitations in accuracy. The k-ε model used requires two experimentally attained coefficients which are not adjustable in Flow Simulation. More accurate results could have been attained using software with adjustable parameters. The SolidWorks Technical Reference [7] provides a validation example for flow over a cylinder. The behavior of the separated air flow and oscillating vortex street forming of the cylinder is similar to the expected flow over the aerodynamic helmets. Figure 2 compares the SolidWorks computational results and experimental data. Aerodynamic helmets normally operate at a Reynolds Number of about 1.0E-5. According to Figure 2 this suggests the SolidWorks Simulation results used for the helmet design are subject to some error. Despite this shortcoming, the Flow Simulations software was used and should provide sufficiently accurate results given the comparative nature of the analysis. The mesh size used was limited by the available computer RAM, but the models were simplified enough to allow this memory to provide accurate flow simulations.

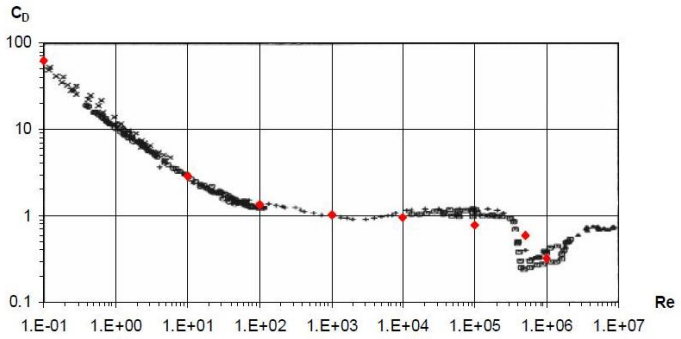

(FIGURE 2)
The cylinder drag coefficient predicted by Flow Simulation (red diamonds) in comparison with the experimental data from the SolidWorks Technical Reference [7]

COMPUTATIONAL FLOW SOLVER AND PROCESS

The commercial CFD code, SolidWorks Flow Simulation, was used to calculate drag forces. The software was implemented as-is and default turbulence model setting were used. Flow Simulation solves the Navier-Stokes equations. These equations are solved on a rectangular computational mesh using the cell-centered finite volume method. The modified Leonard's QUICK method is used to approximate the spacial derivatives with second-order accuracy and the time derivatives with first-order accuracy. The Favre-averaged Navier-Stokes equations are used to predict flow in turbulent regions. The time averaged equations introduce additional terms, the Reynolds stresses, which require the use of addition equations to close the

system. This software closes the system by using a high Reynolds Number k-ε turbulence model which uses the transport equations for turbulent kinetic energy and its dissipation rate [7]. The k-ε model requires two experimentally attained coefficients which are not adjustable in Flow Simulation. Laminar and Turbulent flows near walls are characterized by the Modified Wall Function approach. The simulations were run for unsteady flow to capture oscillating vortex formation. A physical run time of two seconds was used which allowed the drag force to settle into a steady periodic oscillation. Drag force data was averaged over 0.5 physical seconds to compensate for the periodic force oscillation. The adaptive mesh feature of Flow Simulation was enabled which refined the mesh in highly turbulent regions every 0.5 seconds. A grid independent mesh was assured when the periodic force oscillation was not disturbed by the final mesh refinement at a physical run time of 1.5 seconds.

2-D COMPUTATIONAL FLOW ANALYSES

Initial computational models of the two dimensional (2-D) air flow over the symmetric airfoil shape that forms the base of the production helmet were performed. Examining the 2-D flow provided insight into the behavior of the airflow while requiring minimal processor time. The effects of truncation lengths and base modifications were also examined in 2-D. Performing the initial computational runs in 2-D allowed rapid results and provided useful information for the 3-D design.

Modeling Method

The symmetric airfoil shape that forms the base of the production helmet was modeled in SolidWorks. SolidWorks Flow Simulation, using the default solver settings, was used to calculated drag forces. The CFD software uses a one cell thick computational domain to simulate 2-D flow. A high level of initial automatic mesh size was used which also enabled the adaptive mesh function. Due to the expected unstable flow conditions a physical run time of 3 seconds was selected and force results were averaged over 0.5 seconds. Simulations for the production profile, truncation lengths, splitter plate modification, base triangle modification, and base cavity modification were performed. From this data optimal truncation lengths and trailing edge modifications were established.

Results

Production Helmet: The 2-D production helmet shape was tested at three velocities; 8.9 m/s (20 MPH), 11.2 m/s (25 MPH), and 13.4 m/s (30 MPH). As expected the flow separates from the helmet and forms an oscillating Karman vortex street wake. An alternating pattern of a large vortex forming on the tapering rear section of the helmet and then moving down and shedding off the trailing edge developed; this can be seen in Fig 3.

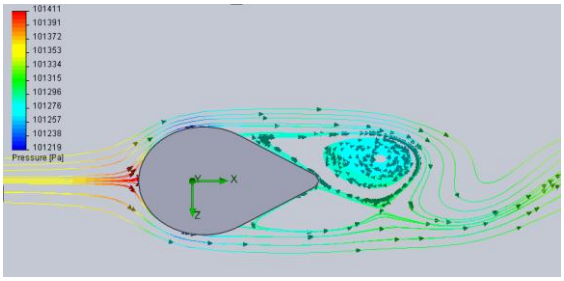

(FIGURE 3)
PRODUCTION HELMET FLOW VISUALIZATION

At 11.2 m/s the production helmet has a coefficient of drag of 0.59 and the 2-D section experiences a total drag force of 0.30 N with a shear drag force of 0.005 N. This finding demonstrates that 98.5 percent of the drag is caused by form drag, while only 1.5 percent is a result of friction drag. Given the Reynolds number, of 100,000, this result was expected. The large low pressure vortices that form on the back section of the helmet significantly contribute to the drag force. Reducing the size and forcing these vortexes to quickly shed could reduce the drag coefficient. Without significantly changing the shape of the helmet or employing a means of complex boundary layer control, keeping the airflow attached is not feasible.

Truncation Optimization: The helmet cross-sectional coefficient of drag was measured as the helmet was progressively truncated to examine the effects of reduced helmet length on drag. The coefficient of drag versus truncation length can be seen in Fig. 4.

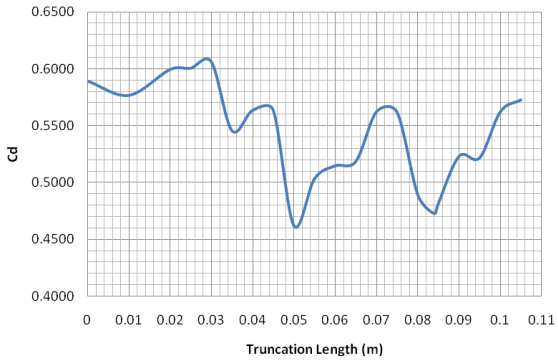

(FIGURE 4)
COEFFICIENT OF DRAG VS TRUNCATION LENGTH

Figure 4 shows distinct truncation lengths of 0.5 m and 0.85 m that result in the lowest coefficients of drag. The length of the helmet affects the size and shedding speed of the vortexes. At truncation lengths of about 0.5 m and 0.85 m the helmet geometry forms smaller vortexes on the blunt trailing edge that are shed quickly. This results in a lower coefficient of drag. The 0.5 m truncation would be the optimal length for reducing drag coefficient but the 0.85 m truncation length was selected. This length has a slightly higher drag coefficient but would present a reduced frontal area if the helmet were rotated 90 degrees into the air stream. Figure 5 shows air flow over the 0.85 m truncation length. The vortex, which is significantly smaller than the vortex formed on the full length helmet, can be seen forming on the helmet.

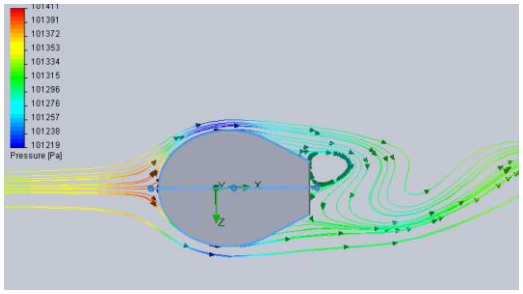

(FIGURE 5)
TRUNCATED HELMET FLOW VISUALIZATION

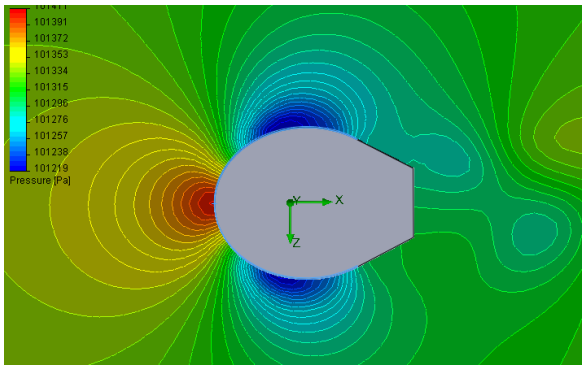

(FIGURE 6)
TRUNCATED HELMET PRESSURE DISTRIBUTION

Figure 6 shows the pressure distribution around the truncated helmet. The increased pressure, compared to the full length helmet, can be seen on the rear portion. In order to verify that this optimal truncation length, which was found at 11.2 m/s, would also be optimal at other expected velocities, the truncation length versus Drag coefficient tests were performed at two other velocities. Figure 7 shows very similar changes to drag coefficient as the helmet is shortened for multiple velocities. These results showed that a helmet optimized at 11.2 m/s would also be optimized for velocities of 8.9 and 13.4 m/s.

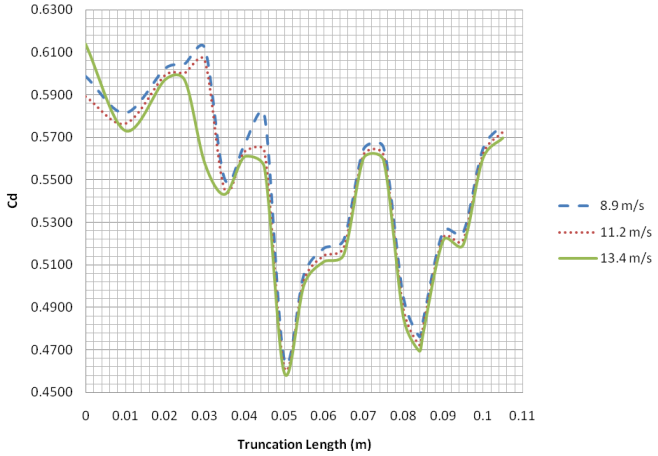

(FIGURE 7)
COEFFICIENT OF DRAG VS TRUNCATION LENGTH

Trailing Edge Modifications: The drag effects of select trailing edge modifications; multiple splitter plates, a base triangle, and multiple base cavities were tested. Figure 8 shows the splitter plate modification, which increased the coefficient of drag when added to the optimized truncation. The splitter plate stabilized the low pressure vortex allowing it to build significantly before being shed therefore reducing the pressure on the trailing edge and increasing drag.

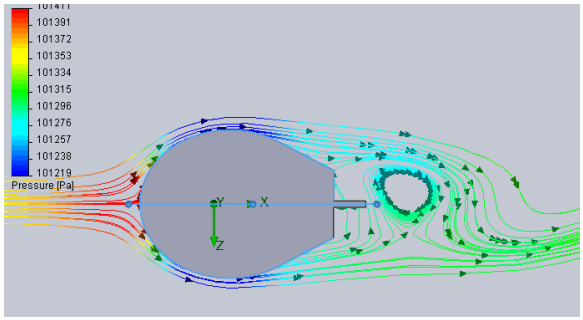

(FIGURE 8)
TRUNCATED HELMET WITH SPLITTER PLATE FLOW VISUALIZATION

Figure 9 shows the base triangle modification. This modification reduced the pressure on the trailing edge by causing a smaller vortex to form on one side of the trailing edge and quickly shedding off.

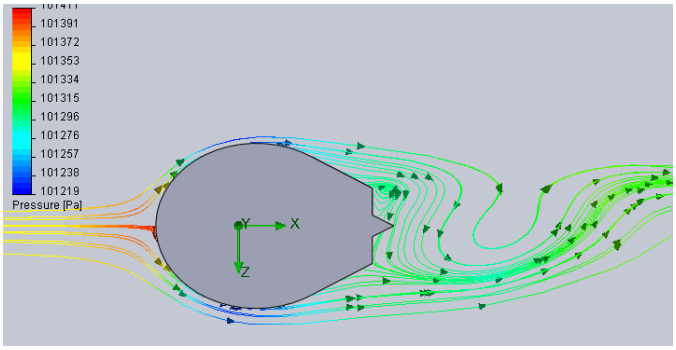

(FIGURE 9)
TRUNCATED HELMET WITH BASE TRIANGLE FLOW VISUALIZATION

Figure 10 shows the optimal trailing edge modification, a base cavity with a 0.0025 m trailing edge thickness. This base cavity has the maximum depth possible without removing structural material from the helmet. This trailing edge modification results in the formation of small vortexes that are quickly shed and result in the lowest coefficient of drag of all the tested geometries.

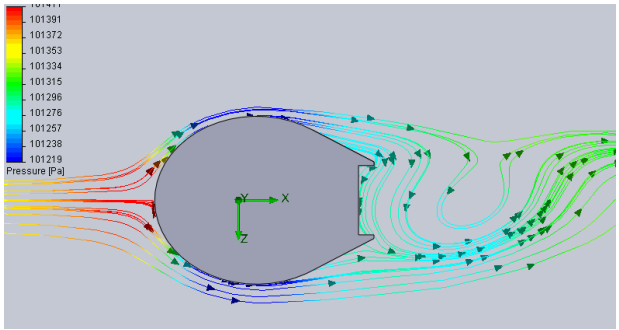

(FIGURE 10)
HELMET WITH BASE CAVITY FLOW VISUALIZATION

Conclusion: The 2-D computational data provided an understanding of the flow patterns over the helmet and insight into the major causes of drag. Given the geometry and the Reynolds number, the flow separates from the helmet and develops an oscillating vortex street as expected. The majority of the drag force is a result of the pressure drag induced by this separation and vortex formation. It was also found that the aerodynamic performance was not only maintained but improved upon by truncating the shape. There are distinct optimal truncation lengths that are not dependent on speed in the velocity ranges that are applicable to the helmet design. A rectangular base cavity with a distinct trailing edge width was shown to further reduce the coefficient of drag. From these results it was predicted that the 3-D production helmet could be truncated with a square base cavity and the coefficient of drag could be reduced. The 2-D model's optimal truncation length was not a function of velocity and it was expected that the 3-D model would behave similarly.

3-D DESIGN AND COMPUTATIONAL ANALYSIS

The air flow over a three dimensional (3-D) model of the production helmet on a head was simulated and the effects of pitch angle on drag forces were examined. The optimal truncation length to apply to the production helmet and the effects of trailing edge modifications were studied. The optimized "improved" helmet was then tested at various pitch angles to compare its performance with the production helmet.

Modeling Method

The production helmet on a head was modeled in SolidWorks and tested with default solver settings in SolidWorks Flow Simulation. A high level of initial automatic mesh was used which also enabled the adaptive mesh function. Figure 11 shows a cross-section of the adapted mesh used for the simulations on the improved helmet at a pitch angle of 0 degrees. This mesh had 2.6E5 grid points. The final mesh sizes varied a small amount between simulations resulting for the use of the adaptive mesh feature. Due to the expected unstable flow conditions a physical run time of 2 seconds was selected and force results were averaged over 0.5 seconds. Simulations for the production helmet, truncation lengths, and trailing edge modification were performed. Using this data a helmet that had a reduced coefficient of drag at 11.2 m/s and at a pitch angle of zero degrees was designed. The production and improved helmet were tested at multiple angles of attack to compare the performance of each helmet when the athlete drops his or her head. In figures that compare drag and pitch angle, drag will be presented in dimensional form in order to show the combined effects of changes in drag coefficient and frontal area.

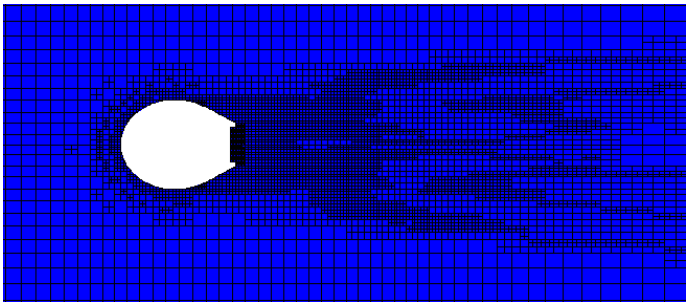

(FIGURE 11)
Cross-section of the final adapted mesh for the improved helmet and a 0 degree pitch angle

Results

Production Helmet: Initially the helmet was modeled and placed on a 3-D scan of a human head for computational testing as can be seen in Fig. 12.

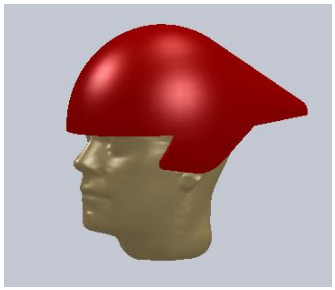

(FIGURE 12)
PRODUCTION HELMET AND HEAD MODEL

This model looked quite realistic but presented meshing problems. The complex geometry of the human head model required a fine mesh, and therefore significant RAM, which limited the mesh available to capture the air flow effects around the helmet. When simulations of this model were run the unsteady flow around the helmet was not modeled correctly. The mesh around the head could have been manually modified to mend this error but reducing the geometric complexity of the helmet and head provided an easier solution to the problem. Given the comparison between the production and the improved helmets, a simplified head model should not significantly alter the results. The simplified helmet and head model can be seen in Fig. 13.

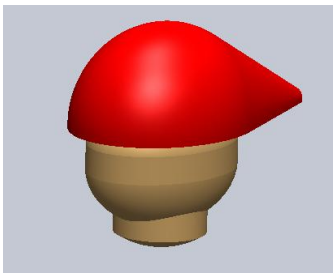

(FIGURE 13)
SIMPLIFIED PRODUCTION HELMET AND HEAD MODEL

The simplified production helmet was tested at 11.2 m/s and showed an alternating vortex street developing around the sides of the helmet and a mostly steady separated flow over the top. Due to the asymmetry of the flow over the top of the helmet an alternating vortex street was not expected here. The production helmet and head model have a coefficient of drag of 0.28. Given the similarities in the flow around the sides of the 3-D helmet and the 2-D shape it was expected that similar truncations and trailing edge modifications would improve the production helmet.

Truncation Optimization: The helmet and head coefficients of drag were measured as the helmet was progressively truncated to examine the effects that the reduced helmet length had on drag for the 3-D model. The coefficient of drag versus truncation length can be seen in Fig. 14. Figure 14 shows a distinct truncation length of 0.9 m, which results in a lower coefficient of drag then the full length helmet. This optimal length significantly reduces the overall helmet length and will reduce the frontal area of the helmet at

low pitch angles to improve head down performance. The air flow over the helmet and head can be seen in Fig. 15.

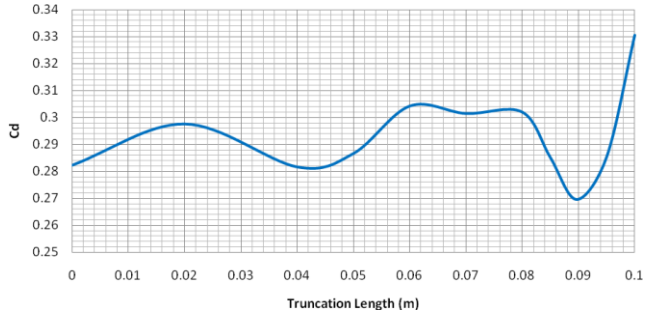

(FIGURE 14)
COEFFICIENT OF DRAG VS TRUNCATION LENGTH, 11.2 M/S, 0 DEGREE PITCH ANGLE

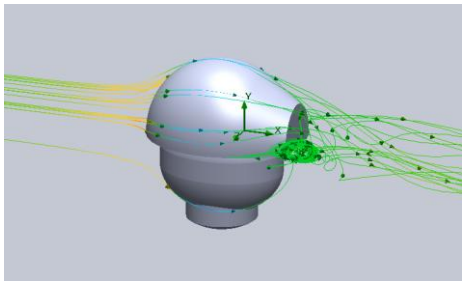

(FIGURE 15)
TRUNCATED HELMET FLOW VISUALIZATION

Trailing Edge Modifications: The drag effects of select trailing edge modifications that could not be modeled in 2-D and the base cavity were tested on the optimized truncated 3-D helmet. The effect of adding vents to the base cavity was tested. The flow can be seen in Fig. 16. The geometry showed an increase in drag forces. In the flow visualization it appears the vents increase the size of the low pressure vortex that forms on the side of the helmet resulting in the drag increase.

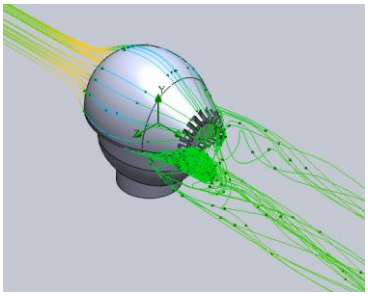

(FIGURE 16)
VENTED BASE CAVITY FLOW VISUALIZATION

Like the 2-D simulations a maximum depth base cavity with a specific trailing edge thickness produced the lowest coefficient of drag. The optimal trailing edge thickness can be seen in Fig. 17. At a velocity of 11.2 m/s and a 0 degree pitch angle the improved helmet shows a 6 percent decrease in coefficient of drag compared to the production helmet.

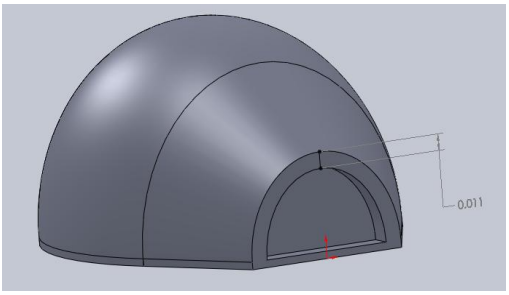

(FIGURE 17)
OPTIMAL TRAILING EDGE THICKNESS

Pitch Angle Testing: After the optimal geometry for minimizing drag at a zero degree pitch angle was determined the effects that the shorter helmet had on drag forces at multiple pitch angles were tested. The drag forces were tested on the production and improved helmet for angles 0 to -90 every 15 degrees. Figure 18 shows the result of these tests by comparing drag force and pitch angle.

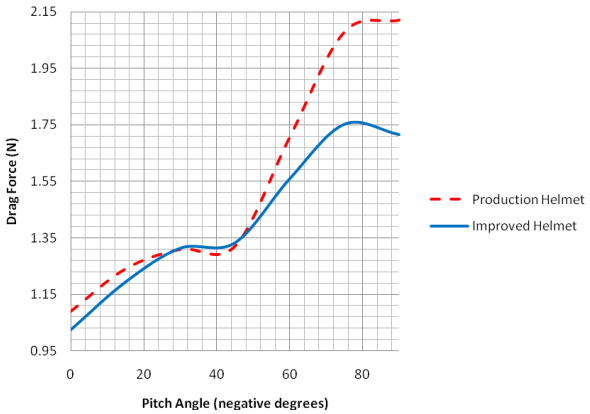

(FIGURE 18)
DRAG FORCE VS PITCH ANGLE

The improved helmet shows a significantly lower drag force at pitch angles of 0 to -25 degrees and at angles from -50 to -90 degrees. At pitch angles near -40 degrees the production helmet has slightly lower drag (less than 1 percent) compared to the improved helmet. In this region the coefficient of drag of the improved helmet is slightly higher than the production helmet and the decrease in frontal area has not yet had an effect.

Conclusion: Significant simplifications to the 3-D model geometry were required to allow a fine enough mesh in the turbulent separated flow region to achieve accurate results. By truncating the simplified 3-D production model and applying a base cavity the drag force was reduced. Similarly to the 2-D simulations, the truncation length and cavity size control the size and shedding speed of the alternating vortexes that form on the sides of the helmet. The percent reduction in drag is significantly less when compared to the 2-D model because of the flow that comes over the top of the helmet. This flow does not form distinct vortexes and is not significantly altered by the truncation or base modification. For the majority of pitch angles the improved helmet shows a significant reduction in drag force.

WIND TUNNEL VERIFICATION OF COMPUTATIONAL RESULTS

In order to verify the computational results, the production and improved helmet were tested at three pitch angles and four air velocities in a wind tunnel. These experimental wind tunnel tests were only performed once. The results from these tests were compared to those from the computational simulations.

Method

The University of Colorado Denver Mechanical Engineering wind tunnel was used to perform the verification tests. The wind tunnel has an 18 inch by 18 inch test area and uses a parallel plate dynamometer capable of measuring drag and lift forces. The dynamometer digitally displays three decimal places in kgf. The dynamometer was manually calibrated using the manufacturer provide balance rod and weight. After manual calibration the force measurement is accurate to 0.01 kgf (0.1 N). Dynamic pressure, vacuum pressure, atmospheric pressure, and atmospheric temperature were recorded for each run and were used to calculate air velocities. Two scale models, the production helmet and the improved design, were tested. These models were scaled to block less than 10 percent of the cross sectional area of the wind tunnel while not requiring speeds in excess of 50 m/s to maintain similitude. The two helmets were tested once at multiple speeds and at pitch angles of 0 degrees, -45 degrees, and -90 degrees. The data attained from the wind tunnel testing were used to examine the drag area versus air speed behavior and used to compare the drag forces at changing head pitch angles.

Results

Input Turbulence Comparison: The computational model requires an input turbulence to drive the turbulence model. Before wind tunnel testing was performed the computational results' sensitivity to input turbulence were tested. Input, or air stream turbulence, in the wind tunnel is not known and cannot be adjusted. If the computational results are significantly altered by changes in input turbulence then the computational results and experimental results cannot be compared accurately. The input turbulence used for the helmet design, was 0.1 percent, which is the default value in SolidWorks Flow Simulation. Input turbulence values of 0.2 percent and 1.0 percent were tested on both helmet designs. These tests were performed at 0 degrees, -45 degrees, and -90 degrees. Figure 19 shows the drag force at 0.2 percent input turbulence compared to the default 0.1 percent input turbulence. This figure shows little difference in the computational results at the 0.1 percent and 0.2 percent input turbulences across the pitch angles.

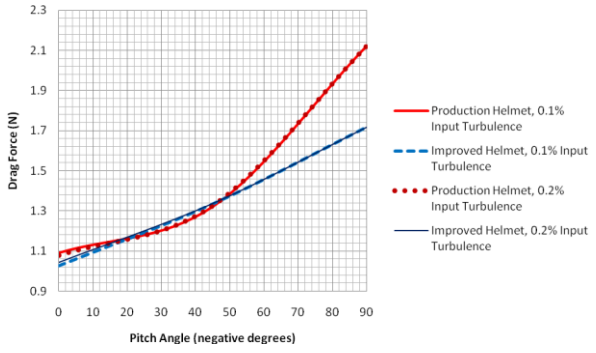

(FIGURE 19)
DRAG FORCE VS PITCH ANGLE,
INPUT TURBULENCE COMPARISON

Figure 20 shows the drag force at 1.0 percent input turbulence compared to the default 0.1 percent input turbulence. This figure shows a significant drag difference at a zero degree pitch angle but similar results at a -45 and -90 degree pitch angles. This result is expected as the increased input turbulence increases the boundary layer turbulence. This moves the airflow separation point farther down the model and reduces form drag. This phenomenon is only apparent at a pitch angle of 0 degrees when the models are somewhat streamlined and not apparent at -45 or -90 degree pitch angles where the sharp edge at the base of the helmet prevents airflow from staying attached. Despite the drag force change at no pitch the comparison between the production and improved helmets is maintained and the wind tunnel results can be confidently compared to the computational data.

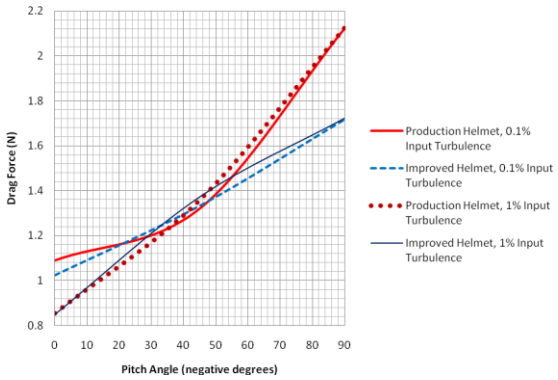

(FIGURE 20)
DRAG FORCE VS PITCH ANGLE,
INPUT TURBULENCE COMPARISON

Wind Tunnel Test Models: A model of the production and the improved helmet designs that could be tested in the wind tunnel were constructed. These models needed to block less than 10 percent of the 18 inch by 18 inch, or 0.209 m², wind tunnel area. This resulted in a maximum allowable model frontal area of 0.021 m². The production helmet at a -90 degree pitch angle has the most frontal area at 0.0596 m². The radius that results in this area is 0.138 m; therefore the model must be scaled down to 59 percent of full size or smaller. In order to maintain Reynolds Number similitude at the air speeds capable of the wind tunnel, using effective frontal area radius, the model must be greater than 27 percent original size. A 40 percent scale was selected as this blocked significantly less than 10 percent of the wind tunnel area and required air speeds easily attained in the wind tunnel while reducing model development costs. The rapid prototyping of the scaled helmet and head models was completed using a Nylon 12 material. The surface finish of the nylon models was quite poor, showing significant material gridding and ridges. High build primer and sanding were used to improve the surface finishes. The models were mounted in the wind tunnel using three ¼"-20 all thread rods. These rods held the models at pitch angles of 0, -45, and -90 degrees and approximately 6 inches forward of the dynamometer. The mounting rods attached to ¼"-20 studs mounted in the back of each head model.

Wind Tunnel Testing: The drag forces on the scale models were measured in the wind tunnel. The models were tested at three pitch angles; 0, -45, and -90 degrees, each at four wind tunnel fan motor settings; 30 Hz (about 24 m/s), 40 Hz (about 32 m/s), 50 Hz

(about 41 m/s), and 60 Hz (about 50 m/s). The 60 Hz motor setting resulted in a wind velocity significantly higher than the maximum speeds reached by cyclist and was not included in the comparison or figures. Atmospheric temperature and atmospheric pressure were recorded. These values combined with the dynamic pressure and vacuum pressure for each run were recorded and used to calculate exact air velocity for each run. Drag force results, in kgf, were also recorded for each run. While most angles and velocities exhibited a small amount of side-to-side or vertical vibration, the improved helmet experienced significant oscillating vertical motion at a pitch angle of 90 degree and motor settings of 30 and 40 Hz. The significant motion caused fluctuating drag readings. An approximate average drag force was attained for these runs but is subject to significant error. At a 90 degree pitch angle the coefficient of drag is expected to change linearly with increases in Reynolds Number given the distinct flow separation along the base of the helmet. This expectation combined with the drag force results attained at motor speeds of 50 and 60 Hz was used to correct the data. The corrected and oscillating results can be seen on the various figures.

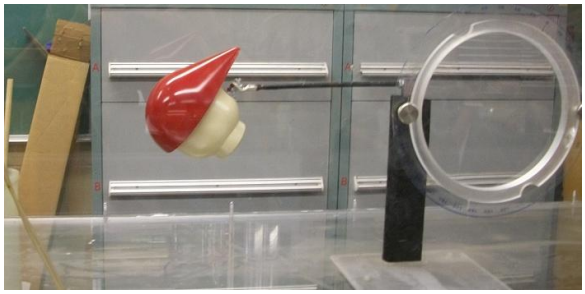

(FIGURE 21)
PRODUCTION HELMET AT PITCH ANGLE = -45 DEGREES

Data: The collected drag data were first used to examine how the model's coefficients of drag changed with Reynolds Number. Figure 22 shows how the coefficient of drag changes with Reynolds Number at a pitch angle of zero degrees. Here we see the coefficient of drag decrease with increased Reynolds Number at about the same rate for both models. At this pitch angle the helmet's geometry is similar to a domed ellipse and the decrease in coefficient of drag with increased velocity matches existing ellipse data. At this pitch angle both helmets have the same frontal area and given the slightly lower coefficient of drag for the production helmet the production helmet would have slightly less drag at this head angle.

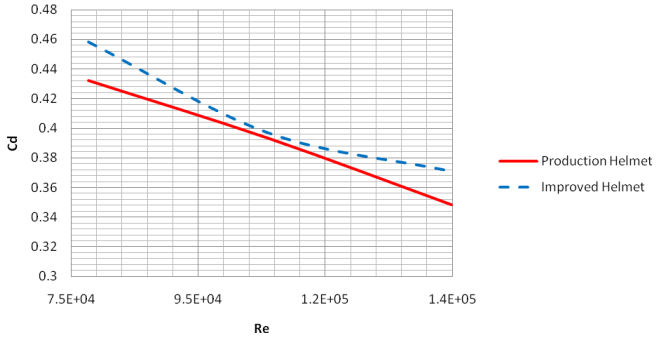

(FIGURE 22)
COEFFICIENT OF DRAG VS REYNOLDS NUMBER
PITCH ANGLE = 0 DEGREES

Figure 23 shows how the coefficient of drag changes with Reynolds Number at a pitch angle of -45 degrees. Here we see the coefficient of drag decrease with increased Reynolds Number at about the same rate for both models but at a slower rate than the zero degree pitch angle. At this pitch angle the helmet's geometry is similar to an ellipse but with some of the air flowing over the sharp edge at the base of the helmet. This separation point acts similarly to the edge of the flat plate and makes the figure more horizontal. At this head angle the production and improved helmet have nearly identical coefficients of drag and given the improved helmet's decreased frontal area at this angle the drag forces on the improved helmet will be lower than on the production helmet.

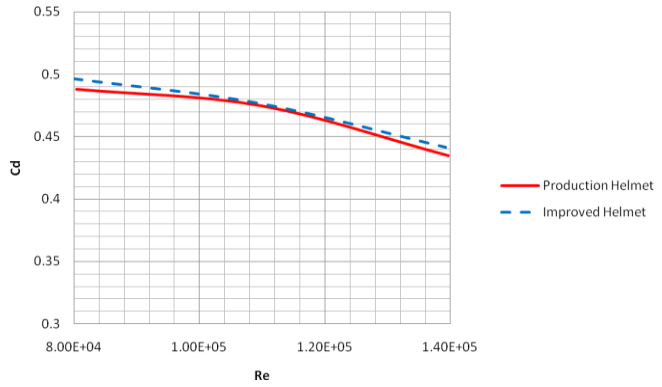

(FIGURE 23)
COEFFICIENT OF DRAG VS REYNOLDS NUMBER
PITCH ANGLE = -45 DEGREES

Figure 24 shows how the drag area changes with velocity at a pitch angle of -90 degrees. Here we see the drag area remains nearly constant as speed is increased. At this pitch angle the helmet's geometry results in flow similar to the flat plate with the airflow separating at the edge on the base of the helmet. This separation point acts similarly to the edge of the flat plate and makes the figure more horizontal. At this head angle the production helmet has a significantly higher coefficient of drag and frontal area as compared to the improved helmet resulting in the improved helmet performing much better than the production helmet.

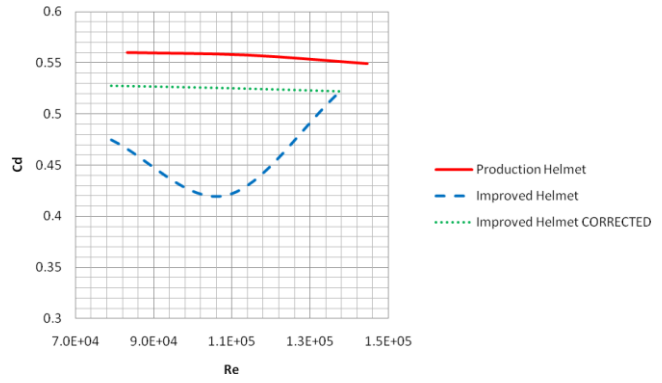

(FIGURE 24)
COEFFICIENT OF DRAG VS REYNOLDS NUMBER
PITCH ANGLE = -90 DEGREES

Figure 25 shows the drag force, which demonstrates the effects of changes in both drag coefficient and frontal area, versus pitch angle for both helmets. Both the computational and experimental results are shown on this figure. The experimental results show higher drag forces than the computational data over nearly the entire range of head pitch angles. As the pitch angle approaches -90 degrees the computational and experimental results match more closely. The wind tunnel results differ from the computational results on average by 17 percent. Despite this difference in the results the comparison between the production and improved helmet is maintained. The production and improved helmet show similar drag forces at pitch angles of 0 and -45 degrees while the improved helmet shows significantly less drag at pitch angles over -45 degrees.

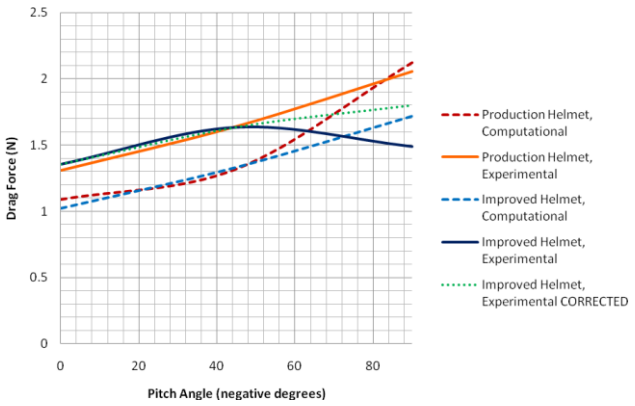

(FIGURE 25)
DRAG FORCE VS PITCH ANGLE
11.2 M/S

Conclusion: The wind tunnel drag force data was, on average, 17 percent different than the computational results. Taking into account the inaccuracies of the computational model and the variations in physical model placement, the wind tunnel and computational results correlated reasonable well. More important than the different force magnitudes is the similarity in comparison between the production and improved helmets in both computational and wind tunnel tests. The experimental results show the same general performance difference between the two helmets. The helmets perform similarly from a pitch angle of 0 to -45 degrees and the improved helmet performs significantly better at pitch angles from -45 to -90 degrees.

GENERAL CONCLUSION

This project investigated the causes of drag on aerodynamic bicycling helmets and presented a solution to improve the performance at multiple head pitch angles. Research examining the performance of current helmets has shown that they do not perform well when the user is not looking directly forward. This investigation was performed in three main steps. First the 2-D flow over the main helmet cross-section was examined and the effects of truncation and trailing edge modification where studied. From this analysis it was concluded that an optimal truncation length could be applied in conjunction with a rectangular base cavity to significantly reduce the helmet's coefficient of drag. Next, these finding were implemented in the design of the 3-D helmet. The improved helmet was optimized in 3-D and compared to the production model. The computational models of the improved 3-D helmet showed lower drag from pitch angle 0 to -25 degrees and significantly lower drag from angle of -50 to -90 degrees. The improved helmet showed a slight higher, less than 1 percent, increase in drag from -30 to -45 degrees. Lastly the computational results were compared to scale models tested in a wind tunnel. The wind tunnel results showed coefficients of drag that differed on average 17 percent from the computational results but showed similar trends in performance compared to pitch angle. Given these results the improved helmet could significantly increase athlete performance.

Future Directions

From the results of this project it is apparent that there is potential for significant improvements in aerodynamic helmet design. A new helmet design, not based on modifying a current model, could implement several unique features. Ducting airflow from the stagnation point through the helmet to vents just past the separation point could keep the air flow attached longer. This used in conjunction with a truncated helmet shaped to divert air around the sides could provide much lower drag. In order to accurately model this design a CFD software package with a more valid turbulence model, possible a k-ω model would be beneficial. This combined with a very fine mesh could provide accurate computational results.

REFERENCES

[1] Alam, F., Subic, A., and Akbarzadeh,A., 2008, "Aerodynamics of Bicycle Helmets," *The Engineering of Sport*, **7**(1), pp. 337-334.

[2] Blair, K., and Sidelko, S., 2008, "Aerodynamic Performance of Cycling Time Trial Helmets," *The Engineering of Sport*, **7**(2), pp. 371-377.

[3] Chabroux, V., Barelle, C., and Favier, D., 2008, "Aerodynamics of Time Trial Bicycle Helmets," *The Engineering of Sport*, **7**(2), pp. 401-410.

[4] Van Dam, C., Kahn, D., and Berg, D., 2008, "Trailing Edge Modifications for Flatback Airfoils," *Sandia Report*, SAND2008-1781.

[5] Wilson, D., 2004, *Bicycling Science, 3rd ed.* Cambridge, MA: Massachusetts Institute of Technology, pp. 110-120 and 174-205.

[6] Jeukendrup, A., 2002, *High-Performance Cycling*, Champaign, IL: Human Kinetics Publishers, Inc, pp. 43-55 and 103-112.

[7] *Governing Equation, Numerical Solution Technique, and Validation Examples*, Flow Simulation 2010 Technical Reference.